EXCITED STATES IN THE NEUTRON RICH NUCLEI ^{46}S AND ^{47}S*

M. Begala[a,b], D. Sohler[a], Z. Elekes[a,b], M.M. Juhász[a]
Y. Utsuno[c,d], T. Otsuka[e,f,g], P. Doornenbal[e], A. Obertelli[e,h,i]
H. Baba[e], F. Browne[e], D. Calvet[i], F. Château[i], S. Chen[e,j,k]
N. Chiga[e], A. Corsi[i], M.L. Cortés[e], A. Delbart[i], J.-M. Gheller[i]
A. Giganon[i], A. Gillibert[i], C. Hilaire[i], T. Isobe[e], T. Kobayashi[l]
Y. Kubota[e,c], V. Lapoux[i], H.N. Liu[h,m], T. Motobayashi[e]
I. Murray[e,n], H. Otsu[e], V. Panin[e], N. Paul[i,o], W. Rodriguez[e,p,q]
H. Sakurai[e,f], M. Sasano[e], D. Steppenbeck[e], L. Stuhl[r,c,a]
Y.L. Sun[h,i], Y. Togano[s,e], T. Uesaka[e], K. Wimmer[f,e], K. Yoneda[e]
N.L. Achouri[t], O. Aktas[u], T. Aumann[h,v], K. Boretzky[v]
C. Caesar[h,v,e], L.X. Chung[w], F. Flavigny[n], S. Franchoo[n]
I. Gašparić[e,x,h], R.-B. Gerst[y], J. Gibelin[t], K.I. Hahn[z,r]
J. Kahlbow[h], D. Kim[e,z,r], T. Koiwai[f], Y. Kondo[α], D. Körper[v]
P. Koseoglou[h,v], J. Lee[k], C. Lehr[h], P.J. Li[β,k], B.D. Linh[w,γ]
T. Lokotko[k], M. MacCormick[n], K. Miki[h,δ], K. Moschner[y]
T. Nakamura[α], S.Y. Park[z,r], D. Rossi[h,v], E. Sahin[ϵ]
F. Schindler[h], H. Simon[v], P.-A. Söderström[h,ζ], S. Takeuchi[α]
H. Törnqvist[h,v], J. Tscheuschner[h], V. Vaquero[η], V. Wagner[h]
S. Wang[β], V. Werner[h], X. Xu[k], H. Yamada[α], D. Yan[β], Z. Yang[e]
M. Yasuda[α], L. Zanetti[h]

for the Sunflower Collaboration

[a]HUN-REN Institute for Nuclear Research, HUN-REN ATOMKI
Pf. 51, 4001 Debrecen, Hungary
[b]University of Debrecen, Doctoral School of Physics, Institute of Physics
Debrecen, Hungary
[c]CNS, University of Tokyo, RIKEN campus, Wako, Japan
[d]Advanced Science Research Center, Japan Atomic Energy Agency, Tokai, Japan
[e]RIKEN Nishina Center, Wako, Japan
[f]University of Tokyo, Hongo, Japan
[g]Instituut voor Kern- en Stralingsfysica, Katholieke Universiteit, Leuven, Belgium
[h]Institut für Kernphysik, TU Darmstadt, Darmstädt, Germany
[i]IRFU, CEA, Université Paris-Saclay, Gif-sur-Yvette, France
[j]University of York, York, UK
[k]The University of Hong Kong, Hong Kong, China
[l]Tohoku University, Sendai, Japan
[m]Key Laboratory of Beam Technology, Beijing Normal University, Beijing, China
[n]IJCLab, IN2P3-CNRS, Université Paris-Saclay, Orsay, France
[o]Laboratoire Kastler Brossel, Sorbonne Université, Paris, France

[p]Universidad Nacional de Colombia, Sede Bogota, Bogotá, Colombia
[q]Pontificia Universidad Javeriana, Bogotá, Colombia
[r]CENS, Institute for Basic Science, Daejon, Republic of Korea
[s]Rikkyo University, Nishi-Ikebukuro, Japan
[t]LPC Caen, ENSICAEN, Université de Caen, CNRS/IN2P3, Caen, France
[u]Royal Institute of Technology, Stockholm, Sweden
[v]GSI, Darmstadt, Germany
[w]Institute for Nuclear Science and Technology, VINATOM, Hanoi, Vietnam
[x]Ruđer Bošković Institute, Zagreb, Croatia
[y]Institut für Kernphysik, Universität zu Köln, Cologne, Germany
[z]Ewha Womans University, Seoul, Republic of Korea
[α]Institute of Science Tokyo, Ookayama, Japan
[β]IMP, Chinese Academy of Sciences, Lanzhou, China
[γ]Vietnam Agency for Radiation and Nuclear Safety, Hanoi, Vietnam
[δ]NSCL, MSU, East Lansing, USA
[ϵ]University of Oslo, Oslo, Norway
[ζ]ELI-NP/IFIN-HH, Bucharest-Măgurele, Romania
[η]Instituto de Estructura de la Materia, CSIC, Madrid, Spain

Received 3 December 2024, accepted 13 February 2025, published online 10 April 2025

Data on the structure of sulphur isotopes close to the neutron drip-line are rather scarce. The excited states of the very neutron-rich ^{46}S and ^{47}S nuclei have been investigated by in-beam gamma-ray spectroscopy at the Radioactive Isotope Beam Factory at the RIKEN Nishina Center. After multi-nucleon knockout reactions on the liquid-hydrogen MINOS target, the $2_1^+ \to 0_1^+$ gamma transition of ^{46}S, already reported in literature, has been confirmed. Additionally, two new gamma rays have been assigned to this isotope and one gamma line has been observed in ^{47}S.

DOI:10.5506/APhysPolBSupp.18.2-A17

1. Introduction

In the last 40 years, the experimental results obtained using radioactive ion beams showed that the shell closures usual in stable nuclei are not valid over the nuclear chart, namely shell closures vanish and new ones develop [1]. Indeed, the neutron-rich nuclei between 30–50 mass numbers exhibit interesting nuclear structure phenomena: the $N = 20$ and 28 neutron shell closures disappear at larger N/Z ratios [2–5] and new sub-shell closures evolve at $N = 32$ and $N = 34$ neutron numbers approaching the neutron drip line [6, 7].

* Presented at the 57$^{\text{th}}$ Zakopane Conference on Nuclear Physics, *Extremes of the Nuclear Landscape*, Zakopane, Poland, 25 August–1 September, 2024.

The neutron-rich sulphur isotopes show several phenomena related to the evolution of the shell closures: while the $N = 20$ shell is closed in ^{36}S, ^{40}S, and ^{42}S show the characteristics of the midshell nuclei, contrary to expectations, in ^{44}S the $N = 28$ shell closure vanishes [8–10]. The nuclei ^{46}S and ^{47}S having 30 and 31 neutrons, respectively, are located between the $N = 28$ and $N = 32$ neutron numbers. Prior information on these nuclei has been rather scarce. Up to our work, only the 2_1^+ state at 952 keV has been identified in ^{46}S [11] and no spectroscopic information was available for ^{47}S. Our aim was to collect in-beam gamma-ray spectroscopy information on ^{46}S and ^{47}S.

We analyzed data collected in the last SEASTAR III campaign, where the setting of the setup was optimized for the production of isotopes around ^{56}Ca. Thanks to the large acceptance of the SAMURAI spectrometer, it was possible to gather data for sulphur nuclei close to the neutron drip-line besides the main goals of the experiment. Previous results obtained in the same experiment can be found in Refs. [12–26].

2. Experimental methods

The experiment was performed at the Radioactive Isotope Beam Factory, operated by the RIKEN Nishina Center and the Center for Nuclear Study of the University of Tokyo. To produce very neutron-rich isotopes with $A \sim 40$–60 mass number, a primary beam of ^{70}Zn with an energy of 345 MeV/u was used. The primary beam impinged on a ^{9}Be target with a thickness of 10 mm. The separation of the secondary cocktail beam was done by the BigRIPS separator [27]. For the identification of the radioactive beam particles, the magnetic rigidity–energy loss–time-of-flight ($B\rho$–ΔE–TOF) method [28] was applied. The velocity was determined from the TOF information provided by the difference in time signals from three plastic scintilators. The $B\rho$ value was obtained by measuring the position and the angle in parallel plate avalanche counters. The atomic number Z was deduced from the ΔE information of the beam particles in an ionization chamber [29]. The incoming particle identification in BigRIPS gated on outgoing ^{46}S and ^{47}S ions can be seen in Fig. 1 (a).

The MINOS liquid-hydrogen target was used to produce the nuclei of interest via multi-nucleon knockout reactions [30, 31]. The length of the target was 151 mm and it was surrounded with a Time Projection Chamber (TPC). The reaction point was reconstructed with a resolution of 5 mm (FWHM) and with an overall efficiency of 65%. The emitted gamma rays were detected by the DALI2$^+$ detector array [32, 33] placed around the MINOS device. It consisted of 226 NaI(Tl) scintillators. The total efficiency of DALI2$^+$ was about 30% at 1 MeV gamma-ray energy. Its energy resolution was about 11% for a moving source with a velocity of 0.6 c.

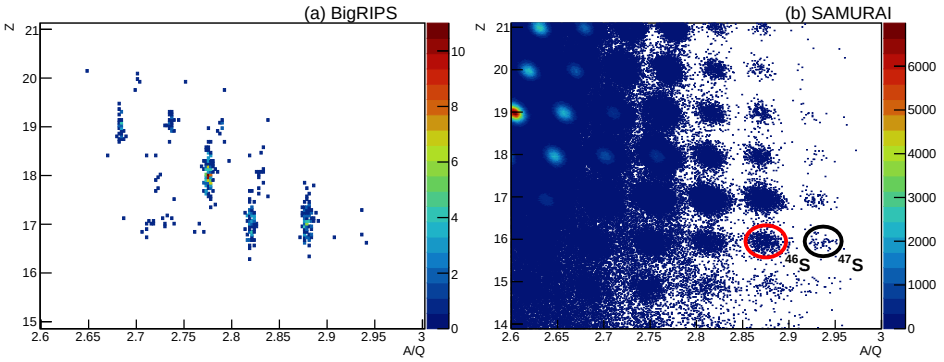

Fig. 1. (Color online) (a) Particle identification plot for incoming ions in BigRIPS, gated on ^{46}S outgoing ions. The different isotopes contributing to the production of ^{46}S are visible. (b) Particle identification in the SAMURAI spectrometer without gating on incoming ions. ^{46}S and ^{47}S are highlighted in red/gray and in black circles, respectively.

The identification of the fragments was performed by the SAMURAI spectrometer [34] based on the $B\rho$–ΔE–TOF information. The $B\rho$ values were deduced from the trajectories of the ions using multi-wire drift chambers. A plastic scintillator wall of 24 segments provided the ΔE and TOF information relative to a plastic detector. The unambiguous identification of the fragments was done by the multi-dimensional fit procedure of the ROOT framework [35]. The particle identification in the SAMURAI spectrometer without gating on incoming ions is shown in Fig. 1 (b). We achieved 7.4σ for separation in Z and 9.4σ for separation in A/Q for the sulphur isotopes.

3. Results

^{46}S was produced by the $(p, 2p1n)$, $(p, 2p2n)$, $(p, 3p2n)$, $(p, 4p2n)$, and $(p, 4p3n)$ multi-nucleon knockout reactions from the ^{48}Cl, ^{49}Cl, ^{50}Ar, ^{51}K, and ^{52}K secondary beams, respectively. Most events originated from the ^{50}Ar with $2p2n$ knockout (43%), ^{49}Cl with $1p2n$ knockout (25%), and ^{48}Cl with $1p1n$ knockout (17%). A total of 380 events related to ^{46}S were collected during the experiment. ^{47}S was populated from similar secondary-beam particles as ^{46}S, mainly from ^{48}Cl, ^{49}Cl, and ^{50}Ar. Although the statistics was very low, we could collect altogether 57 events associated with ^{47}S.

In order to increase the photopeak efficiency of the DALI2^{+} array, an add-back procedure in the analysis was applied. During this procedure, the hits in the adjacent units (< 15 cm) in an event were merged. The emitted gamma rays were Doppler-corrected using the vertex position determined by the TPC and the projected trajectory of the ions entering the target.

Figure 2 shows the Doppler-corrected singles gamma-ray spectrum for ^{46}S including all the reaction channels indicated by $(p, XpYn)$. Three dominant peaks are visible in the spectra: the strongest one is at around 950 keV, and two smaller ones are at around 1500 keV and 2700 keV. The most intense peak corresponds to the gamma line with an energy of 952 keV already identified in ^{46}S [11]. We assign the two additional gamma rays also to ^{46}S.

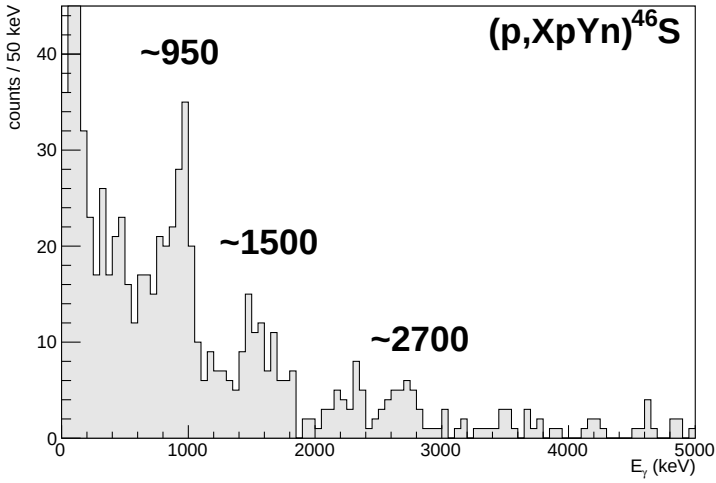

Fig. 2. Doppler-corrected singles gamma-ray spectrum for ^{46}S originating from all the reaction channels using vertex reconstruction and the add-back procedure. The data with shaded area represent the experimental spectrum.

Due to the low statistics, we could not deduce gamma–gamma coincidence relations for the transitions in ^{46}S. In order to gain information on the placement of the gamma rays in the level scheme, spectra gated by different multiplicity conditions were sorted and added together. The multiplicity spectra are presented in Fig. 3. In the spectrum corresponding to multiplicity equal to one ($M = 1$), the peak at an energy of 950 keV is increased as it can be seen in Fig. 3 (a). Accordingly, we confirm that the $\sim$ 950 keV gamma ray decays from the first 2^+ state directly to the 0^+ ground state. In the spectrum belonging to higher gamma-ray multiplicities ($M > 1$), gamma lines corresponding to transitions decaying in a cascade should be more visible. The peaks at about 1500 keV and 2700 keV are more pronounced in this spectrum as it can be seen in Fig. 3 (b). Therefore, we place the two new transitions feeding the first 2^+ state.

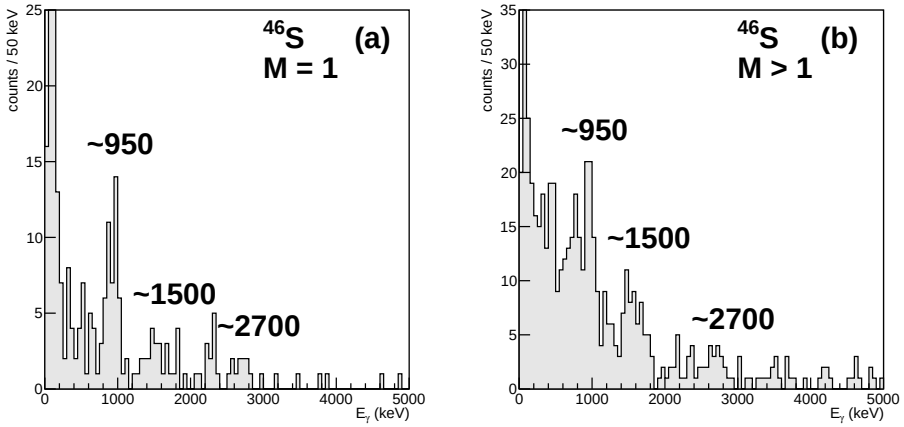

Fig. 3. Doppler-corrected multiplicity gamma-ray spectra for ^{46}S originating from all the reaction channels using vertex reconstruction and the add-back procedure. The data with shaded area represent the experimental spectrum. (a) Events with multiplicity equal to 1 ($M = 1$). (b) Events with multiplicity larger than 1 ($M > 1$).

Despite the low statistics, we could collect counts in the singles gamma-ray spectrum of ^{47}S. A clear peak at about 800 keV was observed in the spectrum. Hence, we assign this gamma ray to ^{47}S.

4. Conclusion

In-beam gamma-ray spectroscopy of ^{46}S and ^{47}S has been performed by multi-nucleon knockout reactions. The already known transition has been confirmed in ^{46}S. Additionally, two new transitions have been assigned to this nucleus. In ^{47}S one gamma ray has been identified. The comparison of the obtained experimental results with theoretical calculations are in progress.

The authors thank the RIKEN Nishina Center accelerator staff for providing the primary beam and the BigRIPS team for the operation of the secondary beam. The development of MINOS has been supported by the European Research Council through the ERC grant No. MINOS-258567. This work was supported by the National Research, Development and Innovation Fund of Hungary (NKFIH), financed by the project with contract No. TKP2021-NKTA-42 and under the K18 funding scheme with project No. K147010. M.B. was partly supported by the EKÖP-24-3 University Research Scholarship Program of the Ministry for Culture and Innovation from the source of the National Research, Development and Innovation Fund of Hungary (NKFIH).

REFERENCES

[1] O. Sorlin, M.G. Porquet, *Prog. Part. Nucl. Phys.* **61**, 602 (2008).
[2] D. Guillemaud-Mueller *et al.*, *Nucl. Phys. A* **426**, 37 (1984).
[3] T. Motobayashi *et al.*, *Phys. Lett. B* **346**, 9 (1995).
[4] B. Bastin *et al.*, *Phys. Rev. Lett.* **99**, 022503 (2007).
[5] S. Takeuchi *et al.*, *Phys. Rev. Lett.* **109**, 182501 (2012).
[6] D. Steppenbeck *et al.*, *Nature* **502**, 207 (2013).
[7] F. Wienholtz *et al.*, *Nature* **498**, 346 (2013).
[8] T. Glasmacher *et al.*, *Phys. Lett. B* **395**, 163 (1997).
[9] D. Sohler *et al.*, *Phys. Rev. C* **66**, 054302 (2002).
[10] C. Force *et al.*, *Phys. Rev. Lett.* **105**, 102501 (2010).
[11] A. Gade *et al.*, *Phys. Rev. Lett.* **102**, 182502 (2009).
[12] M. Cortés *et al.*, *Phys. Lett. B* **800**, 135071 (2020).
[13] M.M. Juhász *et al.*, *Phys. Rev. C* **103**, 064308 (2021).
[14] H.N. Liu *et al.*, *Phys. Rev. Lett.* **122**, 072502 (2019).
[15] S. Chen *et al.*, *Phys. Rev. Lett.* **123**, 142501 (2019).
[16] Y. Sun *et al.*, *Phys. Lett. B* **802**, 135215 (2020).
[17] M.L. Cortés *et al.*, *Phys. Rev. C* **102**, 064320 (2020).
[18] B.D. Linh *et al.*, *Phys. Rev. C* **104**, 044331 (2021).
[19] M. Juhász *et al.*, *Phys. Lett. B* **814**, 136108 (2021).
[20] F. Browne *et al.*, *Phys. Rev. Lett.* **126**, 252501 (2021).
[21] T. Koiwai *et al.*, *Phys. Lett. B* **827**, 136953 (2022).
[22] M. Enciu *et al.*, *Phys. Rev. Lett.* **129**, 262501 (2022).
[23] Z. Elekes *et al.*, *Phys. Rev. C* **106**, 064321 (2022).
[24] S. Chen *et al.*, *Phys. Lett. B* **843**, 138025 (2023).
[25] P.J. Li *et al.*, *Phys. Lett. B* **855**, 138828 (2024).
[26] B.D. Linh *et al.*, *Phys. Rev. C* **109**, 034312 (2024).
[27] T. Kubo *et al.*, *Prog. Theor. Exp. Phys.* **2012**, 03C003 (2012).
[28] N. Fukuda *et al.*, *Nucl. Instrum. Methods Phys. Res. B* **317**, 323 (2013).
[29] K. Kimura *et al.*, *Nucl. Instrum. Methods Phys. Res. A* **538**, 608 (2005).
[30] A. Obertelli *et al.*, *Eur. Phys. J. A* **50**, 8 (2014).
[31] C. Santamaria *et al.*, *Nucl. Instrum. Methods Phys. Res. A* **905**, 138 (2018).
[32] S. Takeuchi *et al.*, *Nucl. Instrum. Methods Phys. Res. A* **763**, 596 (2014).
[33] I. Murray *et al.*, *RIKEN Accel. Prog. Rep.* **51**, 158 (2018).
[34] T. Kobayashi *et al.*, *Nucl. Instrum. Methods Phys. Res. B* **317**, 294 (2013).
[35] ROOT MultiDimFit (accessed August 18, 2022), `https://root.cern.ch/doc/master/classTMultiDimFit.html`